SCISPACE
formerly Typeset

Open access • Journal Article • DOI:10.1007/S00191-017-0504-X

Heterogeneity, spontaneous coordination and extreme events within large-scale and small-scale agent-based financial market models — Source link

Noemi Schmitt, Frank Westerhoff

Institutions: University of Bamberg

Published on: 20 May 2017 - Journal of Evolutionary Economics (Springer Berlin Heidelberg)

Topics: Volatility clustering, Volatility (finance) and Speculation

Related papers:

- Heterogeneous beliefs and routes to chaos in a simple asset pricing model
- Bulls, bears and market sheep
- Herd Behaviour, Bubbles and Crashes.
- Empirical properties of asset returns: stylized facts and statistical issues
- Why a simple herding model may generate the stylized facts of daily returns: explanation and estimation

Share this paper:

View more about this paper here: https://typeset.io/papers/heterogeneity-spontaneous-coordination-and-extreme-events-1uqz7lps2y

ECONSTOR
Make Your Publications Visible.

A Service of

ZBW Leibniz-Informationszentrum Wirtschaft
Leibniz Information Centre for Economics

Schmitt, Noemi; Westerhoff, Frank

Working Paper

Heterogeneity, spontaneous coordination and extreme events within large-scale and small-scale agent-based financial market models

BERG Working Paper Series, No. 111

Provided in Cooperation with:
Bamberg Economic Research Group, Bamberg University

Suggested Citation: Schmitt, Noemi; Westerhoff, Frank (2016) : Heterogeneity, spontaneous coordination and extreme events within large-scale and small-scale agent-based financial market models, BERG Working Paper Series, No. 111, ISBN 978-3-943153-30-9, Bamberg University, Bamberg Economic Research Group (BERG), Bamberg

This Version is available at:
http://hdl.handle.net/10419/144607

Standard-Nutzungsbedingungen:

Die Dokumente auf EconStor dürfen zu eigenen wissenschaftlichen Zwecken und zum Privatgebrauch gespeichert und kopiert werden.

Sie dürfen die Dokumente nicht für öffentliche oder kommerzielle Zwecke vervielfältigen, öffentlich ausstellen, öffentlich zugänglich machen, vertreiben oder anderweitig nutzen.

Sofern die Verfasser die Dokumente unter Open-Content-Lizenzen (insbesondere CC-Lizenzen) zur Verfügung gestellt haben sollten, gelten abweichend von diesen Nutzungsbedingungen die in der dort genannten Lizenz gewährten Nutzungsrechte.

Terms of use:

Documents in EconStor may be saved and copied for your personal and scholarly purposes.

You are not to copy documents for public or commercial purposes, to exhibit the documents publicly, to make them publicly available on the internet, or to distribute or otherwise use the documents in public.

If the documents have been made available under an Open Content Licence (especially Creative Commons Licences), you may exercise further usage rights as specified in the indicated licence.

WWW.ECONSTOR.EU

Mitglied der Leibniz-Gemeinschaft

Heterogeneity, spontaneous coordination and extreme events within large-scale and small-scale agent-based financial market models

Noemi Schmitt and Frank Westerhoff

Working Paper No. 111

June 2016

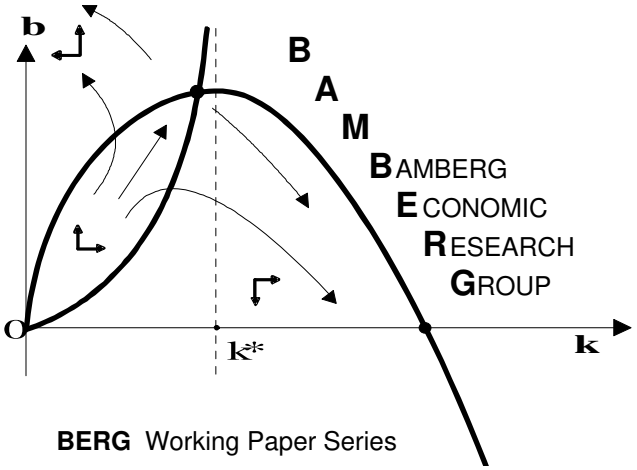

BERG Working Paper Series

Bamberg Economic Research Group
Bamberg University
Feldkirchenstraße 21
D-96052 Bamberg
Telefax: (0951) 863 5547
Telephone: (0951) 863 2687
felix.stuebben@uni-bamberg.de
http://www.uni-bamberg.de/vwl/forschung/berg/

ISBN 978-3-943153-30-9

Redaktion:
Dr. Felix Stübben*

* felix.stuebben@uni-bamberg.de

Heterogeneity, spontaneous coordination and extreme events within large-scale and small-scale agent-based financial market models[☆]

Noemi Schmitt and Frank Westerhoff*

University of Bamberg, Department of Economics,
Feldkirchenstrasse 21, 96045 Bamberg, Germany

Abstract

We propose a novel agent-based financial market framework in which speculators usually follow their own individual technical and fundamental trading rules to determine their orders. However, there are also sunspot-initiated periods in which their trading behavior is correlated. We are able to convert our (very) simple large-scale agent-based model into a simple small-scale agent-based model and show that our framework is able to produce bubbles and crashes, excess volatility, fat-tailed return distributions, serially uncorrelated returns and volatility clustering. While lasting volatility outbursts occur if the mass of speculators switches to technical analysis, extreme price changes emerge if sunspots coordinate temporarily the behavior of speculators.

Keywords: Financial markets, stylized facts, agent-based models, technical and fundamental analysis, heterogeneity and coordination, sunspots and extreme events

JEL classification: C63, D84, G15

1. Introduction

We present a novel agent-based framework to explain a number of important stylized facts of financial markets. A key feature of our approach is that speculators usually determine their orders on the basis of their own individual technical and fundamental trading rules. During these periods, speculators' trading behavior is quite heterogeneous and, as a result, prices oscillate erratically around their fundamental values with alternating periods of low and high volatility. In particular, volatility increases (decreases) and bubbles are likely to occur (vanish) if the mass of speculators relies on technical (fundamental) trading rules. Occasionally, however, speculators

[☆]Presented at the Dynamic Macroeconomics Workshop, Kiel Institute for the World Economy, November 2015. We thank Simone Alfarano, Reiner Franke, Thomas Lux and Christian Proaño for their valuable feedback and comments. The paper also benefitted from a number of constructive remarks from two anonymous referees.

*Corresponding author's email address: frank.westerhoff@uni-bamberg.de

display a spontaneous coordination, caused by salient external events such as investment advice provided by financial gurus. Such exogenously triggered sunspots dissolve heterogeneity among speculators and may lead to extreme market reactions.

Since speculators follow their own individual trading rules, our model may be regarded as a (very) simple large-scale agent-based model. For a review of large-scale agent-based financial market models see, for instance, LeBaron (2006), while important contributions in this direction include LeBaron et al. (1999), Chen and Yeh (2001) and Raberto et al. (2001). However, we show that our model may – assuming, in particular, a large number of speculators – be converted into a small-scale agent-based model. See Hommes (2006) for a review of small-scale agent-based models and Day and Huang (1990), Brock and Hommes (1998), Lux and Marchesi (1999) and Chiarella et al. (2007) for some seminal benchmark contributions.[1] As it turns out, our small-scale agent-based model contains the small-scale agent-based model of Franke and Westerhoff (2012), henceforth referred to as the FW model, as a special case. In this sense, one may argue that our approach also provides a microfoundation for their setup.[2]

Within the FW model, speculators have the choice between a representative technical and a representative fundamental trading rule. These rules contain a deterministic component which captures the essence of technical and fundamental analysis, and a stochastic component which is supposed to take the variety of actual technical and fundamental trading rules into account. Franke and Westerhoff (2012) demonstrate that speculators' switching between a representative (high-noise) technical trading rule and a representative (low-noise) fundamental trading rule generates very reasonable dynamics, including bubbles and crashes, excess volatility, fat-tailed return distributions, serially uncorrelated returns and volatility clustering. However, a weak point of their model is that it fails to generate extreme returns. The reason for this is as follows. Periods of high volatility emerge in that model if the market is dominated by chartists whose orders are mainly generated by a normally distributed shock term. Given the (estimated) value of the standard deviation of this shock term, we know that returns exceeding 7 or 8 percent are very unlikely to occur, although such price changes can indeed be observed in actual financial markets. We show that our small-scale model in which sunspots occasionally coordinate speculators' trading behavior overcomes this problem. Simulations further reveal that our original large-scale agent-based model

[1]The boundary between large-scale and small-scale agent-based models is not clear cut. Examples of models with intermediate complexity include Cont and Bouchaud (2000), Farmer and Joshi (2002) and LeBaron (2012). Moreover, Brock et al. (2005) and Diks and van der Weide (2005) also propose agent-based models with many different trader types and transform these models into small-scale models.

[2]To be precise, Franke and Westerhoff (2012) propose a family of agent-based models and check via an empirical model contest which member of this family has the greatest ability to mimic the behavior of actual financial markets. The model specification DCA-HPM is the winner of this model contest and, for simplicity, we call this model the FW model. Overall, the FW model has a remarkable ability to match the stylized facts of financial markets.

is also able to explain the stylized facts of financial markets.

To be more precise, Franke and Westerhoff (2012) quantify the stylized facts of financial markets with the help of nine moments (summary statistics). Moreover, they define a so-called joint moment coverage ratio, which measures the fraction of simulation runs for which all nine simulated moments jointly drop into the 95 percent confidence intervals of their empirical counterparts. The FW model produces a remarkable JMCR score of about 27 percent. For our setup, we obtain a JMCR score of about 30 percent. However, we modify the JMCR score of Franke and Westerhoff (2012) by adding a tenth summary statistic. Besides the tail index at the 5 percent level, we also take the tail index at the 2.5 percent level into account. In doing so, we seek to find a better way to capture the tail behavior of the distribution of stock market returns. While the modified JMCR score of the FW model drops to about 9 percent (the FW model fails to generate extreme market events), the modified JMCR score of our setup remains around 27 percent. Put differently, our approach does quite well in matching the stylized facts of financial markets and, in particular, produces a more realistic tail behavior of the distribution of the returns than the FW model.[3] As we will see, this result is linked to speculators' sunspot-initiated coordination. In periods in which heterogeneity among speculators breaks down, severe market reactions may emerge. Since such extreme events constitute a high risk for the stability of financial markets, we regard this as an important insight.

To sum up, our paper contributes to the literature by (1) proposing a novel large-scale agent-based financial market model, (2) demonstrating under which conditions such a numerically intensive model can be converted into an analytically tractable small-scale model, and (3) showing that both our small-scale and large-scale models have the ability to match the stylized facts of financial markets. The relevance of our paper may also be seen from the following perspective. An important advantage of large-scale models is that they provide a quite realistic description of the price formation process of actual financial markets. However, the main drawback of large-scale models is that it is frequently difficult to pin down the causalities acting inside these models. In contrast, a very attractive feature of small-scale models is that they usually offer clear-cut analytical insights – albeit at the cost of rather strong simplifying assumptions. One may thus wonder whether it is really legitimate to use small-scale agent-based models to study the dynamics of financial markets, particularly when policy recommendations are concerned. Our paper seeks to provide a bridge between large-scale models and small-scale models. First, we show under which conditions our large-scale model may be converted into a small-scale model. Second, we show that the dynamics

[3]It may be helpful to put these numbers into perspective. Suppose that the moments were independent from each other. Then we would expect the true data-generating process to imply a JMCR score of $0.95^{10} = 0.60$. More conservatively, if we assume that 5 of the 10 moments are independent, then a JMCR score of $0.95^5 = 0.77$ would be obtained.

of our small-scale model is clearly related to its large-scale counterpart. We interpret this evidence also as justification for the use of small-scale models to study the dynamics of financial markets.[4]

The rest of our paper is organized as follows. In Section 2, we briefly present related literature concerned with sunspots and discuss the measurement of extreme events. In Section 3, we present a (very) simple large-scale agent-based financial market model, convert it into a simple small-scale model, and study its relation to the FW model. In Section 4, we briefly recall the stylized facts of financial markets and discuss how they may be quantified and used as a basis for calibrating our model. In Section 5, we bring our framework to the data and evaluate its performance. In Section 6, we conclude our paper and highlight some extensions for future work.

2. Sunspots and extreme events

Since sunspots and extreme market events play a major role in our paper, we want to recap briefly some related literature from these research fields. Recall first that Azariadis (1981) and Cass and Shell (1983) theoretically demonstrate that sunspots, i.e. extrinsic uncertainty in the form of animal spirits, market psychology or prophecies of gurus, may have real macroeconomic consequences. Effects of sunspots are also documented in laboratory experiments. For instance, Duffy and Fisher (2005) study sunspots in financial market experiments in which market participants receive random public signals whether a high or a low price is likely to occur. Although these signals have no bearing on the asset's fundamental value, they observe that market participants use it as a coordination device, thereby affecting the market's price formation process. Marimon and Sunder (1993) show that sequences of sunspot signals may elevate price volatility. Fehr et al. (2012) argue that the impact of sunspots depends on how salient these signals are, whereas Arifovic et al. (2013) and Arifovic and Jiang (2014) conclude that sunspots matter more in periods with greater uncertainty. Within our model, speculators receive random sunspot signals. If they receive such a signal, their behavior is more correlated than usual. It would be straightforward to link the appearance and strength of sunspots to actual market conditions, e.g. to their price and/or fundamental volatility. To make the operating mechanism of our model as clear as possible, we abstain from such possibilities.

It should be noted that the relation between fundamental news and extreme events is rather loose. In an important study, Niederhoffer (1971) examines whether days with significant fundamental news produce bigger stock price changes and reports that major news trigger larger stock

[4]Since the performance of our large-scale model is practically identical to the performance of our small-scale model, the greater heterogeneity of the large-scale model does not seem to be very relevant in explaining the stylized facts of financial markets. As pointed out by an anonymous referee, this suggests that, in order to improve the matching of the stylized facts, one has to consider more trading rules or more complex trading rules or both.

price movements only rarely. Related to this, Cutler et al. (1989) and Fair (2002) check whether days with big stock price changes can be explained by the arrival of significant news. Both studies conclude that many large stock price changes are not associated with any fundamental event. Shiller (2015) argues that extreme market events generally only occur if there is similar thinking among large groups of people. He believes that the news media play an important role in this respect. For instance, certain news, fundamental or non-fundamental, may function as attention grabbers. Shiller (2015) explicitly reports that investment advice provided by financial gurus, which may have no fundamental justification but which are nevertheless transmitted to the general public via popular news stories by the media, can trigger nation-wide attention cascades and thus cause major market movements. Shiller (2015) also scrutinizes the stock market crashes of 1929 and 1987 and concludes that neither of them can be justified from a fundamental economic perspective. Instead, investor psychology, both shaped and enhanced by the media, are major drivers of these events. Inspired by this line of reasoning, we assume within our model that there are sporadic sunspot events that can create spontaneous coordination among speculators. And indeed, our model dynamics reveal that sunspot-initiated coordination, i.e. a temporary breakdown of heterogeneity, can cause major market reactions.

Extreme events, together with their non-negligible frequency, imply that the distribution of stock market returns does not follow a normal distribution. Compared to a normal distribution, the distribution of stock market returns possesses more probability mass in its tails. The outer parts of the distribution of stock market returns are frequently approximated by a power law in the form of $prob(|return| > x) \approx cx^{-\alpha}$, where α is the so-called tail index. The tail index thus provides an opportunity to quantify the fat-tailedness of a distribution. Obviously, a smaller tail index indicates fatter tails. In two authoritative studies, Gopikrishnan et al. (1999) and Plerou et al. (1999) conclude that the tail index of the distribution of returns of individual companies and of major stock market indices is about 3, by which an (inverse) cubic power law is implied. Stanley et al. (2007) provide a fitting example for this outcome. They study the behavior of the S&P500 for a 13-year period and observe $64 = 2^6$ returns greater than 5 standard deviations, $8 = 2^3$ returns larger than 10 standard deviations and $1 = 2^0$ return larger than 20 standard deviations (the latter being Black Monday, 1987). Hence, a doubling of returns reduces their frequency by 2^3.

However, it is difficult to quantify the tail index (see LeBaron 2009 and Alfarano and Lux 2010 for enlightening discussions). A prominent tool to measure the tail index is the Hill tail index estimator (Hill 1975). This estimator requires a choice to be made about the size of the tail region that should be used for the estimation task. Opting for a larger tail region has the advantage that the estimation is based on more data. However, the estimation may also include observations that

do not really belong to the tail region. In this case, the estimation may be biased. In contrast, opting for a smaller tail region implies that the estimation focuses more strongly on the relevant tail region, but also that fewer observations are available for the estimation. In this case, the estimation may suffer from a too high variance. From a practical perspective, tail fractions usually include 2.5 and 5 percent. Against this backdrop, Lux and Ausloos (2002) conclude more cautiously that the tail index of the distribution of returns of major stock markets hovers between 3 and 4. To capture the tail behavior of the distribution of returns, we thus use the tail index at the 2.5 and 5 percent level when we evaluate the performance of our approach.

3. A simple agent-based approach: from large-scale to small-scale

In this section, we introduce a novel agent-based financial market framework to explain the stylized facts of financial markets. We begin this section by previewing the key elements of our approach. In Section 3.2, we present the details of our large-scale agent-based model before converting it into a small-scale agent-based model in Section 3.3. In Section 3.4, we discuss a few special cases of our small-scale agent-based model, including a scenario which corresponds to the FW model.

3.1. Structure and overview of our approach

We consider a single risky asset market which is populated by a fixed number of heterogeneous speculators and a market maker. The fundamental value of the risky asset is constant and known by all market participants. The market maker's task is to mediate the speculators' transactions out of equilibrium and to adjust the price of the risky asset with respect to the current excess demand. If buying orders exceed selling orders, the market maker will increase the price, and vice versa.

Speculators have to decide at the beginning of each period whether to apply technical or fundamental analysis to determine their orders. Technical analysis is based on the assumption that prices move in trends and recommends buying (selling) when prices increase (decrease). According to fundamental analysis, prices may display short-run misalignments but eventually return to their fundamental values. Fundamental analysis thus suggests buying (selling) when markets are undervalued (overvalued).

All speculators follow their own individual technical and fundamental trading rules, which is why these rules are modeled by two components. While one component captures the core of technical and fundamental analysis, the other one reflects the diversity of actual technical and fundamental trading rules. However, the random terms of the latter components are not necessarily

independent. To be precise, we assume that both random terms included in the second parts of technical and fundamental trading rules are multivariate normal distributed with mean vectors of zeros and time-varying variance-covariance matrices. The variance-covariance matrices can take two states, namely one in which the correlation of the random trading signals is low and one in which the correlation is high. The state with the high correlation, referred to as the sunspot case, emerges with a small exogenous probability and is supposed to reflect investment advice provided by financial gurus or other salient external events to which speculators may react. Note that highly correlated random trading signals may increase the excess demand substantially by which, in turn, extreme events may be triggered.

Speculators' choices whether to apply technical or fundamental trading rules are influenced by three socio-economic principles. First, speculators may have a behavioral bias for one of the trading alternatives. Second, they may be subject to herding behavior, i.e. they may prefer to follow the crowd. Third, speculators may evaluate current market circumstances. More precisely, speculators seek to ride bubbles, but they also know that every bubble must eventually burst. Consequently, they perceive fundamental analysis as increasingly attractive as the price of the risky asset moves away from its fundamental value.

Under a few assumptions, including that the number of speculators is large, we can transform our large-scale agent-based model to a small-scale agent-based model. As it turns out, the dynamics of our small-scale model is driven by a three-dimensional first-order nonlinear stochastic dynamical system. Moreover, we show that our small-scale model incorporates the FW model as a special case.

3.2. A (very) simple large-scale agent-based model

Let us turn to the details of our (very) simple large-scale model. The market maker collects all individual orders from speculators and changes the price with respect to the resulting excess demand. By assuming that the market maker uses a log-linear price adjustment rule, we obtain

$$P_{t+1} = P_t + a^M \sum_{i=1}^{N} D_t^i / N, \tag{1}$$

where P_t stands for the log price of the risky asset at time step t, $a^M > 0$ is the market maker's price adjustment parameter, N indicates the total number of speculators and D_t^i represents the order of a single speculator i. Accordingly, the market maker increases (decreases) the price of the risky asset if the sum of the speculators' orders, i.e. the excess demand, is positive (negative). A similar formulation for the market maker's behavior is, for instance, used by Day and Huang

(1990). Note that we divide the excess demand by N to rule out that a change in the total number of speculators affects the price adjustment.

To determine their orders, speculators can either rely on technical or on fundamental analysis. Therefore, we can express the order placed by a single speculator as

$$D_t^i = \begin{cases} D_t^{C,i} & if \quad I_t^i = 1 \\ D_t^{F,i} & if \quad I_t^i = 0 \end{cases}, \tag{2}$$

where $D_t^{C,i}$ and $D_t^{F,i}$ are speculator i's technical and fundamental orders, respectively. As can be seen, speculator i chooses technical (fundamental) trading rules when the indicator function I_t^i takes the value 1 (0). However, this will be explained below in more detail.

Technical analysis seeks to derive trading signals out of past price movements (Murphy 1999). While the core principle of technical analysis is to extrapolate past price trends into the future, there are many different trading rules. To capture at least part of the variety of technical analysis, we specify speculator i's technical trading via two components and obtain

$$D_t^{C,i} = \alpha_t^{C,i}(P_t - P_{t-1}) + \delta_t^{C,i}. \tag{3}$$

The first component of (3) is an explicit trend-extrapolation component and implies that speculators relying on technical analysis go with the current price trend. Parameter $\alpha_t^{C,i}$ represents speculator i's reaction parameter and is assumed to be an independent and identically distributed random variable with a mean of $a^C > 0$ and a finite variance. For instance, $\alpha_t^{C,i}$ may be log-normally distributed so that $\alpha_t^{C,i}$ always remains positive. Alternatively, we may assume that $\alpha_t^{C,i}$ is normally distributed, implying that speculator i sometimes applies contrarian strategies.

The second component of (3) is a random variable that is supposed to take the variety of existing technical trading rules into account.[5] We assume that $\delta_t^C = \{\delta_t^{C,1}, \delta_t^{C,2}, ..., \delta_t^{C,N}\}'$ is multivariate normally distributed with a mean vector μ^C of zeros and a time-varying variance-covariance matrix

[5]Note that there are some contributions in which random terms are added to the demand functions of speculators to capture the diversity of their trading strategies, e.g. in Westerhoff and Dieci (2006), Franke (2010) and Franke and Westerhoff (2016). Moreover, Schmitt and Westerhoff (2014) consider a multi-asset market model in which the random components consist of idiosyncratic, rule-specific, market-wide and general shocks.

Σ_t^C, i.e. $\delta_t^C \sim \mathcal{N}(\mu^C, \Sigma_t^C)$. The variance-covariance matrix is given by

$$\Sigma_t^C = (\sigma^C)^2 \begin{Bmatrix} 1 & \rho_t^C & \dots & \rho_t^C \\ \rho_t^C & 1 & & \vdots \\ \vdots & & \ddots & \rho_t^C \\ \rho_t^C & \dots & \rho_t^C & 1 \end{Bmatrix}, \tag{4}$$

where the correlation coefficients are denoted by

$$\rho_t^C = \begin{cases} \rho^{C,h} & with \;\; prob \; S^C \\ \rho^{C,l} & with \;\; prob \; 1 - S^C \end{cases}. \tag{5}$$

The variance-covariance matrix can take two states. In one state, the correlation between random technical trading signals is low, given by $\rho^{C,l} \geq 0$. This case is referred to as the normal state. In the sunspot case, which represents the other state, the correlation between random technical trading signals is high, given by $\rho^{C,l} < \rho^{C,h} \leq 1$. The probability that a sunspot emerges is denoted by S^C.[6] Note that the assumptions that the mean of $\alpha_t^{C,i}$ is equal to a^C and that the variance of $\delta_t^{C,i}$ is equal to $(\sigma^C)^2$ imply that the trading intensity of technical traders is, on average, of equal size.

Fundamental analysis is based on the premise that asset prices revert towards their fundamental values in the long run (Graham and Dodd 1951). Taking into account digressions from this core principle again, we specify the fundamental demand of speculator i at time step t as

$$D_t^{F,i} = \alpha_t^{F,i}(F - P_t) + \delta_t^{F,i}, \tag{6}$$

where F is the log fundamental value of the risky asset. We assume that F is constant and known by all market participants. Parameter $\alpha_t^{F,i}$ is positive and indicates the strength with which speculator i reacts to the observed mispricing. We assume that $\alpha_t^{F,i}$ are independent and identically distributed random variables with a mean of $a^F > 0$ and a finite variance. For instance, $\alpha_t^{F,i}$ may be drawn from a log-normal distribution or a uniform distribution with positive support.

[6] One example of a sunspot signal could be the investment advice provided by a financial guru. In fact, Shiller (2015, p. 109) argues that Joseph Granville, "a flamboyant market forecaster", may have caused a couple of major market moves. Another example of a sunspot signal could be the emergence of a famous chart signal, such as a clear head-and-shoulders pattern. Analyzing the stock market crash on October 19, 1987, Shiller (2015, p. 118) ventures that two plots which appeared in the Wall Street Journal on the morning of the 1987 crash might have actually triggered the crash. One plot showed the evolution of the Dow in the 1980s, and the other one the evolution of the Dow in the 1920s. Together, both plots suggested that the crash of 1929 might be about to repeat itself. Clearly, chart traders who saw these plots might have thought along similar lines.

For the second part of (6), we assume that $\delta_t^F = \{\delta_t^{F,1}, \delta_t^{F,2}, ..., \delta_t^{F,N}\}'$, $\delta_t^F \sim \mathcal{N}(\mu^F, \Sigma_t^F)$, $\mu^F = \{0, 0, ..., 0\}'$,

$$\Sigma_t^F = (\sigma^F)^2 \begin{Bmatrix} 1 & \rho_t^F & \cdots & \rho_t^F \\ \rho_t^F & 1 & & \vdots \\ \vdots & & \ddots & \rho_t^F \\ \rho_t^F & \cdots & \rho_t^F & 1 \end{Bmatrix} \tag{7}$$

and

$$\rho_t^F = \begin{cases} \rho^{F,h} & with \;\; prob \; S^F \\ \rho^{F,l} & with \;\; prob \; 1 - S^F \end{cases}. \tag{8}$$

The variance-covariance matrix can again take two states. In one state, we have $\rho^{F,l} \geq 0$. In the other one, which emerges with a probability of S^F, we have $\rho^{F,l} < \rho^{F,h} \leq 1$. In the normal state, the $\delta_t^{F,i}$s may reflect, for instance, different interpretations of economic and political news. In the sunspot state, the interpretation of these news is then more aligned.[7] Of course, fundamentalists may also react to investment advice provided by financial (fundamental) gurus or other salient external events, as discussed in Section 2.[8] Assuming that the mean of $\alpha_t^{F,i}$ is equal to a^F and that the variance of $\delta_t^{F,i}$ is $(\sigma^F)^2$ ensures that fundamentalists trade, on average, with equal intensity.

Speculators switch between technical and fundamental analysis with respect to three socio-economic principles.[9] First, speculators may have a predisposition towards technical or fundamental analysis. Second, speculators tend to follow the crowd. Third, speculators react to current market circumstances and increasingly switch towards fundamental analysis when stock prices move away from their fundamental values. Moreover, we follow Franke and Westerhoff (2012) and define a relative fitness function that expresses the fitness of fundamental analysis over technical analysis. Therefore, we obtain

$$A_t^i = \beta^{0,i} + \beta^{H,i}(W_{t-1}^F - W_{t-1}^C) + \beta^{M,i}(F - P_{t-1})^2. \tag{9}$$

[7]For simplicity, we keep the fundamental value in our model constant. In future work, it may be interesting to link the coordination of fundamentalists to the evolution of the fundamental value. For instance, the coordination of fundamentalists may increase with the size of fundamental shocks. We are aware that such a modification stretches the original meaning of sunspots.

[8]The example about the price dynamics of the Dow in the 1920s and 1980s, given in footnote 6, may also influence fundamentalists since it indicates that a fundamental price correction may occur. Whether sunspots affect the behavior of chartists or fundamentalists more strongly is ultimately an empirical question which will be addressed in Section 5. An interesting model extension may be to include sunspots that affect fundamentalists and chartists alike.

[9]The fitness functions in Brock and Hommes (1998) include a constant that may be regarded as a predisposition parameter. In the model of Lux (1995), speculators' rule selection is subject to herding behavior, while in that of de Grauwe et al. (1993), the market impact of fundamental analysis depends on misalignments.

Parameter $\beta^{0,i}$ measures speculator i's predisposition towards fundamental ($\beta^{0,i} > 0$) or technical analysis ($\beta^{0,i} < 0$); parameter $\beta^{H,i} > 0$ determines the strength of speculator i's herding behavior, where W_t^F and W_t^C represent the relative numbers of speculators who follow fundamental and technical analysis at time step t, respectively; and parameter $\beta^{M,i} > 0$ indicates how strongly speculator i reacts to current misalignments. Accordingly, speculator i perceives fundamental analysis as increasingly attractive if his predisposition towards fundamental analysis increases; if the market share of fundamentalists increases; and if the price moves away more strongly from its fundamental value.

The probabilities that speculator i will choose technical or fundamental analysis are determined by using the discrete choice model with multinomial logit probabilities (Manski and McFadden 1981), yielding

$$\pi_t^{C,i} = \frac{exp[\gamma^i A_t^{C,i}]}{exp[\gamma^i A_t^{C,i}] + exp[\gamma^i A_t^{F,i}]} = \frac{1}{1 + exp[\gamma^i (A_t^{F,i} - A_t^{C,i})]} = \frac{1}{1 + exp[\gamma^i A_t^i]} \tag{10}$$

and

$$\pi_t^{F,i} = \frac{exp[\gamma^i A_t^{F,i}]}{exp[\gamma^i A_t^{C,i}] + exp[\gamma^i A_t^{F,i}]} = \frac{1}{1 + exp[-\gamma^i (A_t^{F,i} - A_t^{C,i})]} = \frac{1}{1 + exp[-\gamma^i A_t^i]}, \tag{11}$$

respectively. Note that the relative fitness A_t^i depends on the difference between the fitness of the two trading rules, i.e. $A_t^{F,i} - A_t^{C,i}$, and that $\pi_t^{C,i} + \pi_t^{F,i} = 1$. Equations (10) and (11) imply that the probability of choosing technical (fundamental) trading increases if the relative fitness of fundamental analysis over technical analysis decreases (increases). Parameter γ^i may be regarded as speculator i's intensity of choice; it indicates how strongly speculator i reacts to the trading rules' relative fitness. The higher the intensity of choice, the greater the probability that speculator i will select the trading rule with the higher fitness. For $\gamma^i = 0$, speculator i does not observe any fitness differential and the probability that he will use technical or fundamental analysis is 50 percent. For $\gamma^i = \infty$, fitness differentials are observed perfectly and speculator i selects with a probability of 100 percent the trading rule with the higher fitness.

To keep track of the number of speculators following technical and fundamental analysis, it is convenient to introduce the indicator function

$$I_t^i = \begin{cases} 1 & with \;\; prob \; \pi_t^{C,i} \\ 0 & with \;\; prob \; \pi_t^{F,i} \end{cases}. \tag{12}$$

As can be seen, the indicator function of speculator i takes the values 1 and 0 with the probabil-

ities $\pi_t^{C,i}$ and $\pi_t^{F,i}$, respectively. Since $\pi_t^{C,i}$ ($\pi_t^{F,i}$) represents the probability of selecting technical (fundamental) trading, it can also be stated that $I_t^i = 1$ ($I_t^i = 0$) if speculator i chooses technical (fundamental) analysis to determine his orders. This context was already presented in (2).

Now, the number of speculators relying on technical and fundamental trading rules can easily be determined by

$$N_t^C = \sum_{i=1}^{N} I_t^i \tag{13}$$

and

$$N_t^F = \sum_{i=1}^{N} |I_t^i - 1|, \tag{14}$$

respectively. Of course, the number of chartists plus the number of fundamentalists equals the total number of speculators, i.e. $N_t^C + N_t^F = N$.

The relative numbers of technical and fundamental speculators are therefore given by

$$W_t^C = \frac{N_t^C}{N} \tag{15}$$

and

$$W_t^F = \frac{N_t^F}{N}, \tag{16}$$

respectively. Since the weights of chartists and fundamentalists add up to one, the relative number of speculators who apply fundamental analysis can also be expressed as $W_t^F = 1 - W_t^C$.

3.3. A simple small-scale agent-based model

Let us next explore under which conditions our large-scale model can be converted to a small-scale model. Combining (1)-(3) with (6) yields

$$P_{t+1} = P_t + a^M \{ \sum_{i=1}^{N} I_t^i (\alpha_t^{C,i}(P_t - P_{t-1}) + \delta_t^{C,i}) + \sum_{i=1}^{N} |I_t^i - 1| (\alpha_t^{F,i}(F - P_t) + \delta_t^{F,i}) \} / N. \tag{17}$$

Note first that the sum of correlated normally distributed random variables is normally distributed. Given our assumptions, it follows that $\sum_{i=1}^{N} I_t^i \delta_t^{C,i} = \sigma^C \sqrt{N_t^C} \sqrt{1 + (N_t^C - 1)\rho_t^C} \cdot \epsilon_t^C$ with $\epsilon_t^C \sim \mathcal{N}(0,1)$ and that $\sum_{i=1}^{N} |I_t^i - 1| \delta_t^{F,i} = \sigma^F \sqrt{N_t^F} \sqrt{1 + (N_t^F - 1)\rho_t^F} \cdot \epsilon_t^F$ with $\epsilon_t^F \sim \mathcal{N}(0,1)$.[10] Therefore,

[10] Recall that the variance of the sum of correlated random variables, say $\delta_t^{C,i}$, is given by the sum of their covariances, i.e. $Var(\sum_{i=1}^{N} \delta_t^{C,i}) = \sum_{i=1}^{N} \sum_{j=1}^{N} Cov(\delta_t^{C,i}, \delta_t^{C,j}) = \sum_{i=1}^{N} Var(\delta_t^{C,i}) + 2 \sum_{i=1}^{N-1} \sum_{j=i+1}^{N} Cov(\delta_t^{C,i}, \delta_t^{C,j})$. In our case, random variables $\delta_t^{C,i}$ have equal variances $Var(\delta_t^{C,i}) = (\sigma^C)^2$ and their covariances are given by $Cov(\delta_t^{C,i}, \delta_t^{C,j}) = \rho_t^C (\sigma^C)^2$. Therefore, we can write $Var(\sum_{i=1}^{N} \delta_t^{C,i}) = N(\sigma^C)^2 + 2\frac{N(N-1)}{2} \rho_t^C (\sigma^C)^2 = (\sigma^C)^2 (N + N(N-1)\rho_t^C)$. Accordingly, $Var(\sum_{i=1}^{N} I_t^i \delta_t^{C,i}) = (\sigma^C)^2 N_t^C (1 + (N_t^C - 1)\rho_t^C)$. The same argument applies for the derivation of $Var(\sum_{i=1}^{N} |I_t^i - 1| \delta_t^{F,i}) = (\sigma^F)^2 N_t^F (1 + (N_t^F - 1)\rho_t^F)$.

we obtain

$$P_{t+1} = P_t + a^M \{\sum_{i=1}^{N} I_t^i \alpha_t^{C,i}(P_t - P_{t-1}) + \sigma^C \sqrt{N_t^C}\sqrt{1+(N_t^C-1)\rho_t^C}\ \epsilon_t^C + \sum_{i=1}^{N} |I_t^i - 1| \alpha_t^{F,i}(F - P_t) + \sigma^F \sqrt{N_t^F}\sqrt{1+(N_t^F-1)\rho_t^F}\ \epsilon_t^F\}/N. \tag{18}$$

In order to make our dynamics (virtually) independent of the total number of speculators, let us define $\sigma^C = s^C\sqrt{N}$, $\sigma^F = s^F\sqrt{N}$, $\rho_t^C = X_t^C/N$ with $0 \leq X_t^C \leq N$ and $\rho_t^F = X_t^F/N$ with $0 \leq X_t^F \leq N$.[11] Note that $X_t^C = X_t^F = 0$ implies $\rho_t^C = \rho_t^F = 0$ and that $X_t^C = X_t^F = N$ implies $\rho_t^C = \rho_t^F = 1$. Under these definitions, (18) transforms to

$$P_{t+1} = P_t + \frac{a^M}{N} \{\sum_{i=1}^{N} I_t^i \alpha_t^{C,i}(P_t - P_{t-1}) + s^C\sqrt{N}\sqrt{N_t^C}\sqrt{1+(N_t^C-1)\frac{X_t^C}{N}}\ \epsilon_t^C + \sum_{i=1}^{N} |I_t^i - 1| \alpha_t^{F,i}(F - P_t) + s^F\sqrt{N}\sqrt{N_t^F}\sqrt{1+(N_t^F-1)\frac{X_t^F}{N}}\ \epsilon_t^F\}. \tag{19}$$

Assuming that the number of speculators is large, a number of helpful simplifications and transformations can be made. For instance, the means of the random expressions $\frac{1}{N}\sum_{i=1}^{N} I_t^i \alpha_t^{C,i}$ and $\frac{1}{N}\sum_{i=1}^{N} |I_t^i - 1| \alpha_t^{F,i}$ are given by $W_t^C a^C$ and $W_t^F a^F$, respectively, while their variances converge to zero. Accordingly, (19) simplifies to

$$P_{t+1} = P_t + a^M \{W_t^C a^C (P_t - P_{t-1}) + s^C \frac{1}{\sqrt{N}}\sqrt{N_t^C}\sqrt{1+(N_t^C-1)\frac{X_t^C}{N}}\ \epsilon_t^C + W_t^F a^F (F - P_t) + s^F \frac{1}{\sqrt{N}}\sqrt{N_t^F}\sqrt{1+(N_t^F-1)\frac{X_t^F}{N}}\ \epsilon_t^F\}. \tag{20}$$

Since N is large, the limit of terms $\frac{N_t^C}{N} - \frac{N_t^C-1}{N}$ and $\frac{N_t^F}{N} - \frac{N_t^F-1}{N}$ approaches zero, i.e. we can set $W_t^C = \frac{N_t^C}{N} \approx \frac{N_t^C-1}{N}$ and $W_t^F = \frac{N_t^F}{N} \approx \frac{N_t^F-1}{N}$. This results in

$$P_{t+1} = P_t + a^M \{W_t^C a^C (P_t - P_{t-1}) + s^C\sqrt{W_t^C}\sqrt{1+X_t^C W_t^C}\ \epsilon_t^C + W_t^F a^F (F - P_t) + s^F\sqrt{W_t^F}\sqrt{1+X_t^F W_t^F}\ \epsilon_t^F\}. \tag{21}$$

In the following, we further assume that speculators are homogenous with respect to their rule selection behavior and set $\beta^{0,i} = b^0$, $\beta^{H,i} = b^H$, $\beta^{M,i} = b^M$ and $\gamma^i = c$. Entering these assumptions in (9) and combining with (10) and (12) shows that the indicator function takes the value 1 with

[11] By "virtually independent" we mean that we want to express the dynamical system of our model independently of N. Of course, restrictions $X_t^C \leq N$ and $X_t^F \leq N$ remain, i.e. X_t^C and X_t^F implicitly define a lower limit for N.

a probability of $\pi_t^C = 1/(1 + exp[c(b^0 + b^H(W_{t-1}^F - W_{t-1}^C) + b^M(F - P_{t-1})^2)])$ and 0 otherwise, i.e. I_t^i is binomially distributed. Since the random variable W_t^C is defined by $\frac{N_t^C}{N} = \frac{1}{N}\sum_{i=1}^N I_t^i$, it has a mean of π_t^C and a variance of $\frac{\pi_t^C \pi_t^F}{N}$. Due to our assumption that N is large, the variance of W_t^C vanishes and, thus, we can continue to work with the deterministic equation

$$W_t^C = \frac{1}{1 + exp[c(b^0 + b^H(W_{t-1}^F - W_{t-1}^C) + b^M(F - P_{t-1})^2)]}. \tag{22}$$

Of course, the same applies for W_t^F, resulting in

$$W_t^F = \frac{1}{1 + exp[-c(b^0 + b^H(W_{t-1}^F - W_{t-1}^C) + b^M(F - P_{t-1})^2)]}. \tag{23}$$

Finally, we introduce the auxiliary variable $\tilde{P}_{t+1} = P_t$, which makes it possible to summarize the dynamics of our simple small-scale agent-based financial market model by a three-dimensional first-order nonlinear stochastic dynamical system:

$$\begin{aligned} P_{t+1} = P_t + a^M\{&W_t^C a^C(P_t - \tilde{P}_t) + s^C\sqrt{W_t^C}\sqrt{1 + X_t^C W_t^C}\ \epsilon_t^C + \\ &(1 - W_t^C)a^F(F - P_t) + s^F\sqrt{1 - W_t^C}\sqrt{1 + X_t^F(1 - W_t^C)}\ \epsilon_t^F\}, \end{aligned} \tag{24}$$

$$\tilde{P}_{t+1} = P_t \tag{25}$$

and

$$W_{t+1}^C = \frac{1}{1 + exp[c(b^0 + b^H(1 - 2W_t^C) + b^M(F - P_t)^2)]}, \tag{26}$$

where

$$X_t^C = \begin{cases} X^{C,h} & with\ \ prob\ S^C \\ X^{C,l} & with\ \ prob\ 1 - S^C \end{cases}, \tag{27}$$

$$X_t^F = \begin{cases} X^{F,h} & with\ \ prob\ S^F \\ X^{F,l} & with\ \ prob\ 1 - S^F \end{cases}, \tag{28}$$

$\epsilon_t^C \sim \mathcal{N}(0,1)$ and $\epsilon_t^F \sim \mathcal{N}(0,1)$. In total, this model has 16 parameters. However, a^M and c are scaling parameters and the dynamics does not depend on F. Therefore, there remain 13 parameters to be specified, namely a^C, s^C, a^F, s^F, b^0, b^H, b^M, $X^{C,h}$, $X^{C,l}$, $X^{F,h}$, $X^{F,l}$, S^C and S^F. We stress once again that specifying $X^{C,h}$ and $X^{F,h}$ automatically determines a lower boundary for the total number of speculators. For instance, if $X^{C,h} = 400$, then there are at least $N = 400$ speculators.

3.4. Some special cases of our small-scale model

To improve our understanding of how our small-scale model functions, we explore a few properties of some limiting cases. Let us start with the case in which the stochastic components of technical and fundamental trading rules are not correlated, i.e. $X_t^C = X^{C,l} = X^{C,h} = 0$ and $X_t^F = X^{F,l} = X^{F,h} = 0$. This turns the model's price adjustment equation into

$$\begin{aligned} P_{t+1} &= P_t + a^M\{W_t^C a^C(P_t - P_{t-1}) + s^C\sqrt{W_t^C}\epsilon_t^C + W_t^F a^F(F - P_t) + s^F\sqrt{W_t^F}\epsilon_t^F\} \\ &= P_t + a^M\{W_t^C a^C(P_t - P_{t-1}) + W_t^F a^F(F - P_t) + \sqrt{W_t^C(s^C)^2 + W_t^F(s^F)^2}\ \epsilon_t\}. \end{aligned} \tag{29}$$

If we assume a perfect correlation between the stochastic components of technical and fundamental trading rules, i.e. $X_t^C = X^{C,l} = X^{C,h} = N$ and $X_t^F = X^{F,l} = X^{F,h} = N$, we obtain

$$\begin{aligned} P_{t+1} &= P_t + a^M\{W_t^C a^C(P_t - P_{t-1}) + s^C W_t^C\sqrt{N}\epsilon_t^C + W_t^F a^F(F - P_t) + s^F W_t^F\sqrt{N}\epsilon_t^F\} \\ &= P_t + a^M\{W_t^C a^C(P_t - P_{t-1}) + W_t^F a^F(F - P_t) + \sqrt{(s^C W_t^C)^2 N + (s^F W_t^F)^2 N}\ \epsilon_t\}. \end{aligned} \tag{30}$$

Finally, recall that $\sigma^C = s^C\sqrt{N}$ and that $\sigma^F = s^F\sqrt{N}$. This turns (30) into

$$\begin{aligned} P_{t+1} &= P_t + a^M\{W_t^C a^C(P_t - P_{t-1}) + \sigma^C W_t^C\epsilon_t^C + W_t^F a^F(F - P_t) + \sigma^F W_t^F\epsilon_t^F\} \\ &= P_t + a^M\{W_t^C a^C(P_t - P_{t-1}) + W_t^F a^F(F - P_t) + \sqrt{(\sigma^C W_t^C)^2 + (\sigma^F W_t^F)^2}\ \epsilon_t\}. \end{aligned} \tag{31}$$

Since the sum of two independent normally distributed random variables is normally distributed, we can summarize the two shock terms in the first lines of (29)-(31) by a single shock term, where $\epsilon_t \sim \mathcal{N}(0,1)$. The derivation of (30) is most easily visible from (20). Using, instead, (24) requires recalling that $1 + NW_t^C \approx NW_t^C$ and that $1 + NW_t^F \approx NW_t^F$.

As it turns out, (31) combined with (26) is identical to the FW model. As already mentioned, the FW model has a remarkable ability to replicate the dynamics of financial markets. One of the key reasons for this outcome is that the variance of the noise term ϵ_t, given by $(\sigma^C W_t^C)^2 + (\sigma^F W_t^F)^2$, depends on time-varying market shares of chartists and fundamentalists, a feature Franke and Westerhoff (2012) call structural stochastic volatility. Note that our paper points out which assumptions need to be made in order to derive the FW model from a more elaborate large-scale model.

Let us compare the price-adjustment equation of the FW model with the one we obtain when speculators' trading signals are not correlated. Random terms ϵ_t^C and ϵ_t^F in (29) are multiplied by $s^C\sqrt{W_t^C}$ and $s^F\sqrt{W_t^F}$, whereas they are multiplied by $\sigma^C W_t^C$ and $\sigma^F W_t^F$ in (31). As a result, the second lines of (29) and (31) show that the variance of the noise term ϵ_t is a linear function

and a quadratic function, respectively, in the market share of chartists. This implies for $s^C = \sigma^C$, $s^F = \sigma^F$ and a given value of W_t^C that the variance of the noise term ϵ_t in (29) is higher than the one in (31). The only exceptions are with $W_t^C = 0$ and $W_t^C = 1$ for which the variances are identical.

The difference between (29) and (30), i.e. the difference between no correlation and perfect correlation of the stochastic components of speculators' trading signals, is that the random components of the technical and fundamental demand are $\sqrt{W_t^C}\sqrt{N}$ and $\sqrt{W_t^F}\sqrt{N}$ times stronger if the model moves from a state with no correlation to a state with perfect correlation. Let us illustrate this using a simple example. Assume that $a^M = 1$, $P_t = P_{t-1}$, $s^C = 1$, $W_t^C = 1$ and $\epsilon_t^C = 0.01$. For $X_t^C = X^{C,l} = X^{C,h} = 0$, implying that $\rho_t^C = 0$, the dynamics is characterized by a return of $r_{t+1} = P_{t+1} - P_t = 0.01$. If $X_t^C = X^{C,l} = X^{C,h} = N = 400$, we have $\rho_t^C = 1$ and the same shock yields a return of about 20 percent, i.e. a 20 times intense price change. However, it is not necessary to assume a perfect correlation between chartists' or fundamentalists' stochastic trading signals to obtain realistic returns. In one of our calibrated small-scale models, we have $X_t^C = 20$ with *prob* 0.014 and zero otherwise, while X_t^F is always zero. If we assume that $N = 100$, $X_t^C = 20$ implies a mere correlation coefficient of $\rho_t^C = 0.05$, i.e. even a weak sunspot-initiated coordination can lead to severe market events.

4. Stylized facts and model calibration

Since the different model specifications of our approach are designed to explain the stylized facts of financial markets, we begin this section by briefly reviewing some of those properties, namely: (1) bubbles and crashes, (2) excess volatility, (3) fat-tailed return distributions, (4) uncorrelated returns and (5) volatility clustering. Detailed descriptions of the statistical properties of financial markets can be found in Mantegna and Stanley (2000), Cont (2001) or Lux and Ausloos (2002). To make our results comparable to the study of Franke and Westerhoff (2012), our exposition rests on the behavior of the S&P500 stock market index with $T = 6858$ daily observations from January 1, 1980 to March 15, 2007.

In Figure 1, we illustrate the dynamics of the S&P500 for the considered period. The top panel shows the evolution of the daily log stock price. Note that the time series has been detrended and centered around zero. As can be seen, the evolution of stock prices show both strong price appreciations and major crashes. The second panel of Figure 1 displays the daily returns of the S&P500 between 1980 and 2007. Apparently, prices fluctuate strongly and there are extreme price changes up to 23 percent. The central panels of Figure 1 illustrate the fat tail property. On the left-hand side, we plot the cumulative distribution of normalized returns (black line),

i.e. returns are divided by the standard deviation, together with the cumulative distribution of standard normally distributed returns (gray line) on a log-log scale. The panel clearly shows that extreme returns occur more frequently than warranted by the normal distribution, which indicates that the distribution of empirical returns possesses more probability mass in the tails. As it is common to quantify the fat tail property by estimating the Hill tail index, we plot the Hill tail index estimator as a function of the largest returns (in percent) on the right-hand side. At the 2.5 and 5 percent levels, for instance, the Hill tail index is given by 3.48 and 3.25, respectively. Note that the lower the value for the tail index, the fatter the tails. In the bottom two panels of Figure 1, we display the autocorrelation functions of raw and absolute returns, respectively. Since the gray lines represent 95 percent confidence bands, the raw return time series shows correlation coefficients that are not significant for almost all lags. However, the autocorrelation coefficients of absolute returns are clearly significant for more than 100 lags, evincing temporal persistence in volatility and volatility clustering.

Besides determining the ability of our framework to match the stylized facts, we also want to compare the performance of our different model versions with that of the FW model, which is why we follow Franke and Westerhoff (2012) and use the same summary statistics (moments) to measure the statistical properties of the S&P500. They use the mean value of absolute returns, the Hill tail index at the 5 percent level, the first-order autocorrelation coefficient of raw returns and the autocorrelation coefficients of absolute returns for lags 1, 5, 10, 25, 50 and 100 to quantify the overall volatility, the fat tail property, the absence of autocorrelations in raw returns and the long memory in absolute returns, respectively. As pointed out in Section 2, however, we add the Hill tail index at the 2.5 percent level as a tenth statistic in order to capture the tail behavior of the distribution of returns in more detail. These ten summary statistics are presented together with the lower and upper boundaries of their 95% conficence intervals in Table 1. The computation of the confidence intervals follows also Franke and Westerhoff (2012); see their Appendix A and Table A.1 for further information.[12]

To evaluate how well their model is able to match the moments, Franke and Westerhoff (2012) used the concept of a joint moment coverage ratio, which measures the fraction of simulation runs for which all nine simulated moments jointly are contained in the 95 percent confidence intervals of their empirical counterparts. For instance, with their estimated parameter setting they obtained a JMCR(09) score, i.e. a JMCR score based on nine summary statistics, of about 27 percent. Since

[12]Since our calibration strategy relies on the moments' confidence intervals, different methods to compute these intervals may lead to different parameter settings, different performance values and, eventually, different model rankings.

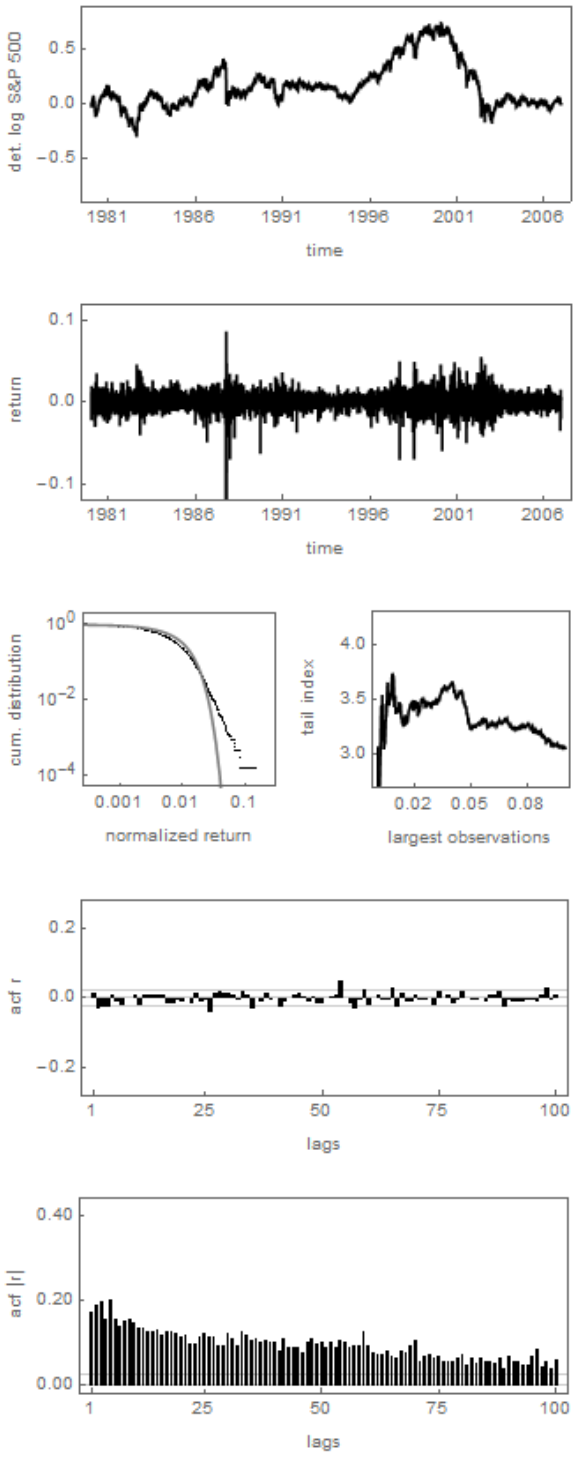

Figure 1: The dynamics of the S&P500 between 1980 and 2007. The panels show from top to bottom the evolution of the S&P500, the returns, the cumulative distribution of normalized returns, the Hill tail index estimator as a function of the largest returns and the autocorrelation functions of raw and absolute returns, respectively.

	V	$\alpha_{2.5}$	$\alpha_{5.0}$	$ac\ r_1$	$ac\ \lvert r_1\rvert$
Measured	0.713	3.481	3.251	−0.008	0.193
Lower bound	0.672	3.020	2.990	−0.042	0.106
Upper bound	0.754	4.090	3.710	0.0270	0.280
	$ac\ \lvert r_5\rvert$	$ac\ \lvert r_{10}\rvert$	$ac\ \lvert r_{25}\rvert$	$ac\ \lvert r_{50}\rvert$	$ac\ \lvert r_{100}\rvert$
Measured	0.187	0.159	0.128	0.112	0.074
Lower bound	0.142	0.118	0.095	0.074	0.041
Upper bound	0.231	0.200	0.162	0.148	0.105

Table 1: Empirical moments of the S&P500. The table contains estimates of the volatility V, the tail index $\alpha_{2.5}$ and $\alpha_{5.0}$, the autocorrelation function of raw returns $ac\ r$ for lag 1 and the autocorrelation function of absolute returns $ac\ |r_i|$ for lags $i \in \{1, 5, 10, 25, 30, 100\}$. The second and third lines show the lower and upper boundaries of the 95% confidence intervals around the empirical statistics that are reported in the first lines. Estimates are based on a time series ranging from January 1, 1980 to March 15, 2007 that contains 6858 daily observations. For more details on the computation of these statistics, see Franke and Westerhoff (2012).

we added a tenth summary statistic, we try to find parameter settings for our model versions that maximize the JMCR(10) score.

Given the number of model parameters, it is unfortunately impossible to achieve a true maximization of the JMCR(10) score. To see the problem, note that a plain grid search procedure requires many simulations to determine the parameters of one of our model versions. For instance, if one varies all seven parameters of the FW model in 100 discrete steps and computes each time the JMCR score on the basis of 5000 simulation runs, one needs to generate $5000 \cdot 100^7$ simulation runs to estimate this model. If we seek to determine all 13 parameters of our approach in the same way, $5000 \cdot 100^{13}$ simulation runs have to be generated, i.e. the computational effort, which is already high, increases by a factor of 100^4. The parameter settings of our model versions have thus been determined on the basis of what may be called a human-guided grid search procedure. To be more precise, we execute smaller grid searches in a certain parameter neighborhood and after analyzing the results (using our economic intuition), we turn to a more promising parameter neighborhood. Initially, we used 500 repetitions to compute the JMCR(10) score and when the results stabilized, we increased this number to 5000. We are therefore unable to rule out the existence of better performing parameter settings. Put differently, the fit reported in our paper may be regarded as a lower boundary of the possible performance of our approach.[13] As we will see, the fit we obtained in this way appears to be quite satisfactory. A drawback of our informal calibration strategy is, however, that we have to be careful when comparing the performance of different models, in particular when ranking models with respect to their JMCR(10) scores.

[13]For other studies which rely on the method of simulated moments to estimate small-scale agent-based models see, for example, Winker et al. (2007), Franke (2009a) or Chen and Lux (2015).

5. Model dynamics and performance

In this section, we discuss a number of different specifications of our agent-based financial market framework. To be able to appreciate our results, we start with the FW model, i.e. a setup that has no sunspots. As already mentioned, Franke and Westerhoff (2012) estimated this model, given by (31) and (26), based on the JMCR(09) criterion. The parameter estimates are presented in Table 2; a summary of the model's performance is given in Table 3; and a typical simulation run is depicted in Figure 2.

	a^C	s^C	σ^C	a^F	s^F	σ^F	b^0	b^H	b^M	$X^{C,h}$	S^C	$X^{F,h}$	S^F
FW	1.50	-	2.147	0.120	-	0.708	−0.336	1.839	19.671	-	-	-	-
S-C0	1.50	1.707	-	0.132	0.552	-	−0.336	2.317	19.671	20	0.014	0	0
S-0F	1.50	1.610	-	0.144	0.460	-	−0.336	2.354	19.671	0	0	82	0.013
S-CF	1.50	1.653	-	0.138	0.545	-	−0.336	2.446	19.671	20	0.009	40	0.005

Table 2: Parameter settings for different model specifications. The first, second, third and fourth lines present the paramter setting for the FW model, a small-scale model in which only chartists obtain sunspot signals, a small-scale model in which only fundamentalists obtain sunspot signals and a small-scale model in which all speculators obtain sunspot signals, respectively. The remaining parameters are $a^M = 0.1$, $c = 1$, $F = 0$, $X^{C,l} = 0$ and $X^{F,l} = 0$.

The simulation run in Figure 2 contains 6750 daily observations. Since the design of Figure 2 is identical to that of Figure 1, our simulation can be compared directly with the dynamics of the S&P500. The first panel of Figure 2 shows that the FW model gives rise to bubbles and crashes – although this is not accounted for by the estimation procedure. As can be seen, the log price fluctuates erratically around its log fundamental value ($F = 0$) and there are extended periods in which the market is either undervalued or overvalued. The second panel of Figure 2 shows that the market is quite volatile, similar to the S&P500. In addition, there are a couple of volatility outbursts. In the left panel of the third line of Figure 2, we observe more probability mass in the tails of the returns' distribution than in the case of a normal distribution. The right panel shows again estimates of the tail index for increasing tail fractions. For instance, we observe a tail index of about 3.38 for a tail size of 5 percent. The penultimate panel of Figure 2 shows that almost all autocorrelation coefficients are insignificant, i.e. the development of log prices is close to a random walk. The final panel of Figure 2 shows that autocorrelation coefficients of absolute returns are highly significant and decay slowly as the lag length increases.

The functioning of the FW model may be explained as follows. Due to the heterogeneity of speculators' trading rules, prices evolve quite randomly. If the mass of speculators favors technical analysis, volatility increases and bubbles are likely to occur. As the price runs away from its fundamental value, however, speculators rely increasingly on fundamental analysis. As a result, the market calms down and approaches its fundamental value. This in turn can trigger a new wave of chartism and the onset of the next financial crisis. Note that volatility outbursts imply a

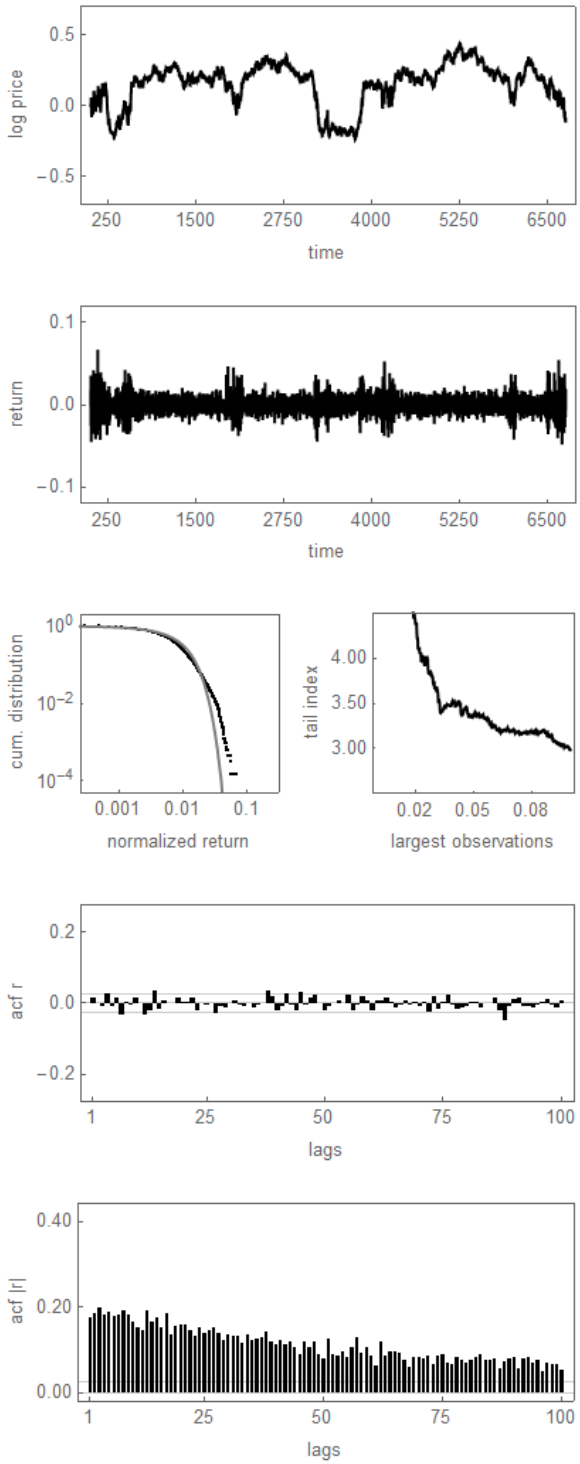

Figure 2: The dynamics of the FW model. The panels show from top to bottom the evolution of the log price, the returns, the cumulative distribution of normalized returns, the Hill tail index estimator as a function of the largest returns and the autocorrelation functions of raw and absolute returns, respectively.

number of higher returns, which lead to a fat-tailed return distribution.

The first column of Table 3 gives a more precise picture of the performance of the FW model. Taking the original nine moments of Franke and Westerhoff (2012) into account, the model produces a JMCR(09) score of about 27 percent. Also the matching of the individual nine moments is quite satisfactory. For instance, the autocorrelation coefficients of the absolute returns are in the 95 percent confidence intervals of their empirical counterparts in 73.1 to 98.7 percent. However, the model seems to have a problem in producing extreme returns. This can already be seen by comparing Figures 1 and 2. While the returns of the S&P500 may be up to 23 percent, the returns of the FW model hardly exceed the 7 percent level. As a result, the distribution of returns possesses less probability mass in the (outer) tails; and estimates of the tail index, based on a tail fraction of 2.5 percent, are unusually high. This is also clear from Table 3. The tail index at the 2.5 percent level is within the 95 percent confidence interval of its empirical counterpart in less than 30 percent of the simulation runs. As a result, the JMCR(10) score, at 9 percent, is much lower than the JMCR(09) score, namely 27.2 percent.

	FW	S-C0	S-0F	S-CF	L-CF	L-CFA
JMCR(10) score	0.090	0.268	0.240	0.273	0.257	0.263
JMCR(09) score	0.272	0.300	0.300	0.318	0.310	0.306
V	0.565	0.525	0.508	0.542	0.538	0.542
$\alpha_{2.5}$	0.291	0.855	0.638	0.788	0.778	0.796
$\alpha_{5.0}$	0.692	0.925	0.601	0.859	0.860	0.863
$ac\ r_1$	0.974	0.972	0.983	0.976	0.976	0.979
$ac\ \lvert r_1\rvert$	0.987	0.997	0.985	0.994	0.996	0.994
$ac\ \lvert r_5\rvert$	0.927	0.884	0.747	0.846	0.854	0.837
$ac\ \lvert r_{10}\rvert$	0.888	0.956	0.930	0.956	0.954	0.947
$ac\ \lvert r_{25}\rvert$	0.785	0.884	0.905	0.897	0.899	0.897
$ac\ \lvert r_{50}\rvert$	0.853	0.874	0.904	0.890	0.880	0.893
$ac\ \lvert r_{100}\rvert$	0.731	0.735	0.809	0.750	0.730	0.752
Average score	0.769	0.861	0.801	0.850	0.847	0.848

Table 3: Performance of different model specifications. The first, second, third, fourth, fifth and sixth columns present the performance of the FW model, a small-scale model in which only chartists obtain sunspots, a small-scale model in which only fundamentalists obtain sunspots, a small-scale model in which chartists and fundamentalists obtain sunspots, a large-scale model in which chartists and fundamentalists obtain sunspots and a large-scale model that extends the L-CF model, respectively. The respective JMCR(09) and JMCR(10) scores are presented in the first two lines. The table also contains the fractions of individual moments' matching and their respective average score. Estimations are based on 5000 simulation runs.

How well does our small-scale model with sunspots, i.e. setup (24) to (28), perform? The second column of Table 3 provides a first answer. The acronym S-C0 stands for a small-scale model in which only chartists receive sunspot signals. The parameters of this model, given in the second row of Table 2, were obtained in our attempt to maximize the JMCR(10) score. As can be seen, the JMCR(10) score is about 27 percent, while the JMCR(09) score is as much as around

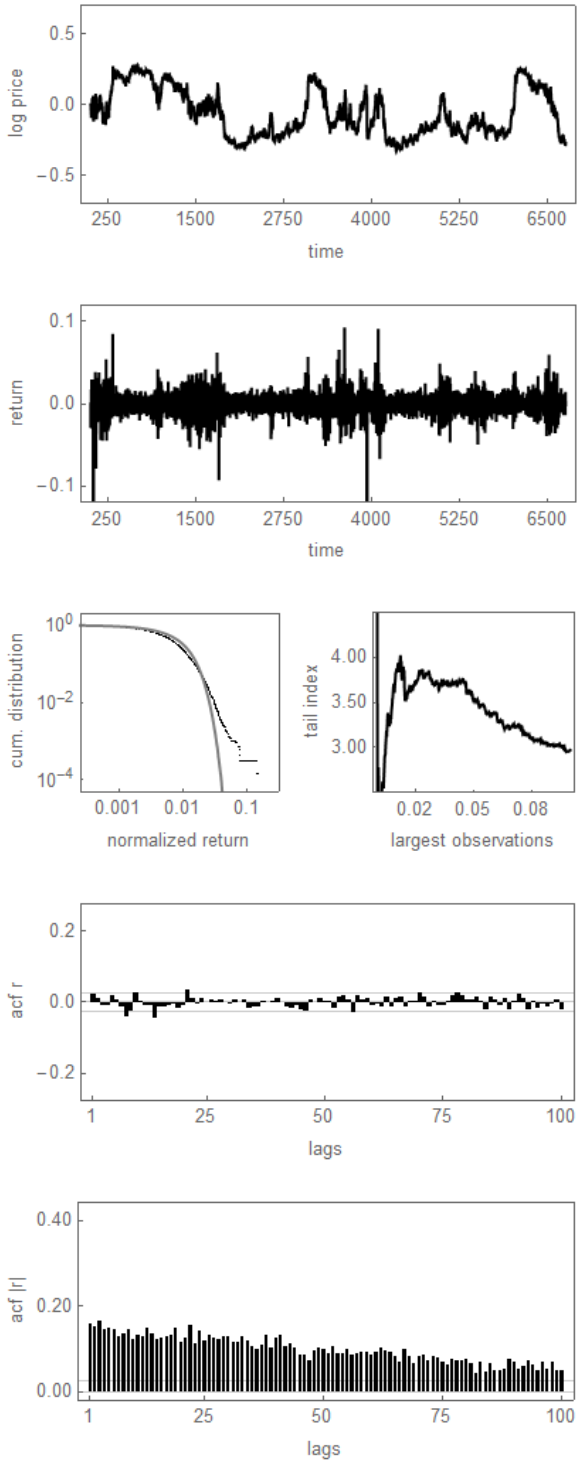

Figure 3: The dynamics of a small-scale model in which only chartists obtain sunspots (S-C0 model). The panels show from top to bottom the evolution of the log price, the returns, the cumulative distribution of normalized returns, the Hill tail index estimator as a function of the largest returns and the autocorrelation functions of raw and absolute returns, respectively.

30 percent. The main reason for this increase in performance is the much better fit of the two tail indices. The tail index at the 2.5 percent level is now matched in about 86 percent of cases, whereas the tail index at the 5 percent level is matched in about 93 percent of cases.[14]

Figure 3 provides an example of the dynamics of the S-C0 model. A comparison of Figures 1 to 3 immediately reveals that the S-C0 model does a better job at matching the behavior of the S&P500 than the FW model. In particular, the S-C0 model generates a number of extreme returns which are quite comparable to what we observe for the S&P500. As a result, there is more probability mass in the tails of the return distribution, and estimates of the tail index appear more realistic. Of course, we have to take into account that the S-C0 model has two more parameters than the FW model. Due to the strong performance increase, however, we believe that this disadvantage is more than compensated for by the increase in performance of the S-C0 model. The functioning of the S-C0 model is similar to that of the FW model, except that infrequent sunspots temporarily coordinate speculators' behavior. In these periods, the excess demand may escalate which, in turn, triggers major market reactions.

Figure 4 illustrates the dynamics of a model specification in which only fundamentalists receive sunspot signals. The parameter setting for this model, labeled S-0F, is given in the third row of Table 2; an overview about its performance is presented in the third column of Table 3. As can be seen, this model version is also able to replicate the stylized facts of financial markets quite well. While we have to be careful in ranking our different model versions, it is clear that the S-0F model outperforms the FW model. However, the S-0F model seems to drop slightly behind the S-C0 model. With respect to the parameter settings of the S-0F and S-C0 models, we note that $X^{F,h} = 82$ in the S-0F model is about four times higher than $X^{C,h} = 20$ in the S-C0 model. One reason for this is that the magnitude of the random demand component of fundamentalists in the S-0F model, namely $s^F = 0.460$, is only about a fourth of that of chartists in the S-C0 model, given by $s^C = 1.707$.

The fourth column of Table 3 presents the dynamics of an almost fully specified small-scale model, i.e. now chartists and fundamentalists receive sunspot signals. The parameters of this model, which we call the S-CF model, are reported in the last row of Table 2; Figure 5 visualizes its dynamics. Note that the correlation between the stochastic components of trading rules is still zero in the normal state. As to be expected, the performance of the S-CF model exceeds that of the S-C0 model and the S-0F model, albeit only moderately. Whether one prefers specification S-C0,

[14]By paying greater attention to the tail behavior of the distribution of returns, these values may be further improved. However, we determine the model parameters by trying to maximize the JMCR(10) score, and in this sense there is a trade-off between matching of two tail indices and matching the other eight summary statistics.

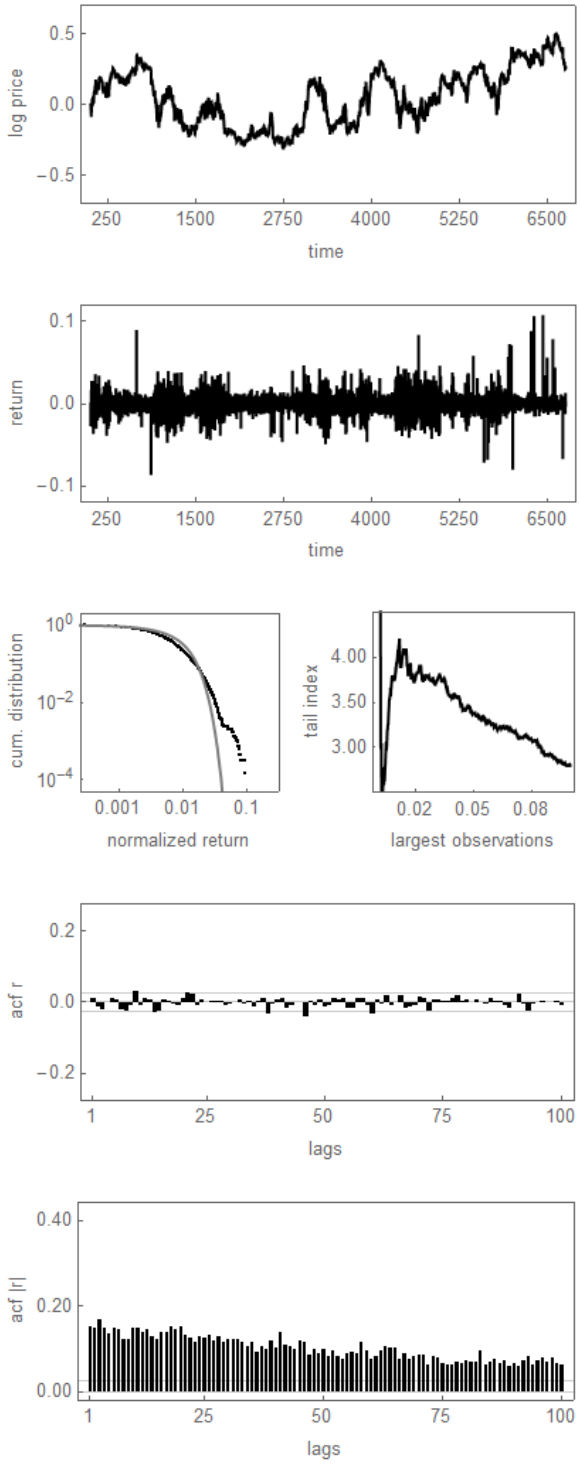

Figure 4: The dynamics of a small-scale model in which only fundamentalists obtain sunspots (S-0F model). The panels show from top to bottom the evolution of the log price, the returns, the cumulative distribution of normalized returns, the Hill tail index estimator as a function of the largest returns and the autocorrelation functions of raw and absolute returns, respectively.

S-0F or S-CF is a matter of taste – and it is beyond the scope of our paper to correct the JMCR criterion for the number of model parameters. Besides relying on the pure JMCR score, one may also take the economic implications of the S-CF setup into account. From an economic perspective, it may seem more reasonable to assume that both chartists and fundamentalists react to external signals, particularly because speculators switch between these trading rules. A comparison of Figures 3 and 4 furthermore reveals that extreme events emerge in the S-C0 model when chartists dominate the market and volatility is relatively high and in the S-0F model when fundamentalists dominate the market and volatility is relatively low. Due to its parameter setting, the S-CF model – see Figure 5 – usually produces extreme returns when chartists dominate the market and occasionally when fundamentalists dominate the market. In any case, the performance of our model versions is quite satisfactory. This is also apparent when examining the model's average moment matching. For instance, the average score of the S-C0, S-0F and S-CF model is 86.1, 80.1 and 85 percent, respectively.

Let us now proceed with the performance of our large-scale models. The fifth column of Table 3 summarizes the performance of the L-CF model. This model corresponds to our original large-scale model, represented by (1) to (16), in which chartists and fundamentalists receive sunspot signals. The simulation analysis is based on $N = 100$ speculators. It should be clear that $N = 100$ is a rather small number and that the dynamics of the large-scale model approaches the dynamics of the small-scale model as the number of speculators increases (part of the randomness created by speculators obviously washes out as N increases). At the beginning of each time step, each speculator makes a probabilistic choice with respect to which trading rule should be followed, where the probabilities of being a chartist or a fundamentalist are due to (10) and (11). In addition, we vary the reaction parameters of speculators' technical and fundamental trading rules. To be precise, $\alpha_t^{C,i}$ and $\alpha_t^{F,i}$ are drawn from uniform distributions $\alpha_t^{C,i} \sim \mathcal{U}(1.125, 1.875)$ and $\alpha_t^{F,i} \sim \mathcal{U}(0.099, 0.165)$, respectively, which corresponds to a ± 25 percent interval around the means $a^C = 1.5$ and $a^F = 0.132$. As can be seen, the performance of the L-CF model is similar to that of the S-CF model. Our final experiment is even more encouraging. The L-CFA model extends the L-CF model by additionally assuming that the parameters of the relative fitness (attractive) function are drawn from uniform distributions, i.e. $\beta^{0,i} \sim \mathcal{U}(-0.37, -0.302)$, $\beta^{H,i} \sim \mathcal{U}(2.085, 2.520)$ and $\beta^{M,i} \sim \mathcal{U}(17.704, 21.638)$. Accordingly, these parameters scatter between ± 10 percent around the means $b^0 = -0.336$, $b^H = 2.317$ and $b^M = 19.671$. Note that this extension goes beyond our approximation. Nevertheless, the L-CFA model also obtains a respectable JMCR(10) score of 26,3 percent.

We find it quite encouraging that the performance of our large-scale and small-scale models is

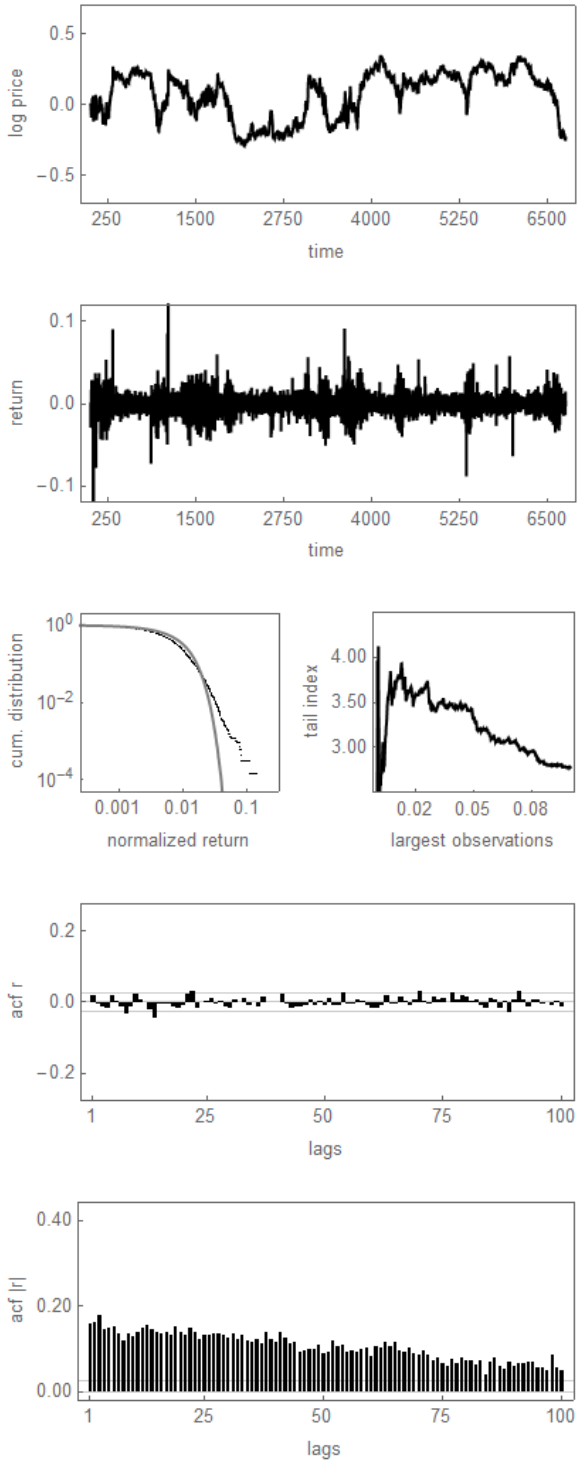

Figure 5: The dynamics of a small-scale model in which chartists and fundamentalists obtain sunspots (S-CF model). The panels show from top to bottom the evolution of the log price, the returns, the cumulative distribution of normalized returns, the Hill tail index estimator as a function of the largest returns and the autocorrelation functions of raw and absolute returns, respectively.

relatively similar. Since simulating our large-scale model is rather time-consuming, it would be virtually impossible to determine its parameters without the help of small-scale models.[15] However, small-scale models help us to calibrate large-scale models. One may also interpret our results in the following way. The use of small-scale models is, for obvious reasons, much more popular than the use of large-scale models. Our analysis suggests that the use of simple prototype small-scale models can be justified since their performance is quite similar to that of more elaborate large-scale models.

6. Conclusions

The dynamics of financial markets can be characterized by bubbles and crashes, excess volatility, fat-tailed return distributions, uncorrelated returns and volatility clustering. The aim of our paper is to explain these intriguing and, from an economic perspective, highly relevant phenomena on the basis of an agent-based financial market framework. Our starting point is a (very) simple large-scale model in which speculators usually follow their own individual technical and fundamental trading rules. Since the mass of speculators switches periodically between technical and fundamental analysis, the market alternates between turbulent and tranquil periods. Another crucial feature of our approach is that sunspot events in the form of infrequent salient external events, such as investment advice provided by financial gurus, may lead to temporary coordination of speculators' behavior. If many speculators trade in the same direction, i.e. if heterogeneity among speculators temporarily breaks down, the excess demand tends to escalate and, consequently, severe market reactions may occur.

Literally speaking, the dynamics of our large-scale model is driven by hundreds of equations. Under a few assumptions, however, the large-scale model can be reduced to a small-scale model. As it turns out, the dynamics of the small-scale model is determined by a three-dimensional first-order nonlinear stochastic dynamical system. Since simulating the small-scale model takes much less time than simulating the large-scale model, we are able to bring our agent-based framework to the data. Overall, we find that our small-scale model has a remarkable ability to match the stylized facts of financial markets. By defining ten summary statistics to capture a number of important stylized facts of financial markets, we are able to compute a so-called joint moment coverage ratio. We find that our small-scale model generates a JMCR(10) score of about 27 percent, i.e. we observe that in about 27 percent of the simulations all ten summary statistics jointly fall into the 95 percent

[15] To give an example, we use Mathematica 10 to simulate our models. The time taken to compute a single time series with 6750 observations increases from about 0.4 seconds to about 45 seconds if we switch from a small-scale model to a large-scale model with 100 speculators, and to about 800 seconds if we set $N = 400$.

confidence intervals of their empirical counterparts. We find it very encouraging that our large-scale model produces a similarly good fit. Since simulating our large-scale agent-based model is quite time-consuming, it would be virtually impossible to determine its parameters without the help of our small-scale model.

Our approach may be extended in various directions.

- First of all, it would be interesting to substitute our informal calibration strategy with a more solid estimation approach. While a fully-fledged JMCR(10) estimation is basically precluded by the large number of model parameters, one may estimate the model by minimizing an ordinary (quadratic) loss function made up of the JMCR(10) score's summary statistics, where for each parameter setting the model would only have to be simulated once (albeit over a very long time horizon to reduce sample variability).[16]

- To make the functioning of our framework as clear as possible, we assume that sunspots emerge with a small exogenous probability. Of course, more could be done with respect to this assumption. For instance, one may assume that sunspots appear in clusters or one could link the probability of a sunspot to current market conditions (sunspots may occur more frequently in turbulent periods). One could even consider modeling the sign of sunspots. For instance, negative (positive) sunspots may appear with a higher probability in extreme bull (bear) markets and trigger fundamental market corrections.

- Alternatively, one could exclude the possibility of sunspots altogether within our framework and model the correlation among the stochastic trading signals of speculators completely endogenously. In Schmitt and Westerhoff (2016), for instance, we show that a time-varying correlation of the stochastic trading signals, coupled to the market's volatility, can lead to volatility clustering, even if speculators do not switch between technical and fundamental trading rules.

- Moreover, it may be worthwhile studying the consequences of alternative fitness functions. For instance, speculators may condition their choice of trading rules on the basis of the rules' past performance.

- Using the large-scale model, one could also track speculators' positions, model their inventory, and study the evolution of their wealth. For example, Franke and Asada (2008) and Franke (2009b) present a quite convincing setup for the inventory management behavior of speculators. Interestingly, they find that, as long as speculators control their inventory not

[16] We thank an anonymous referee for pointing this out.

too aggressively, their positions remain bounded and the effects on the dynamics remain negligible. Against this backdrop, we have, for simplicity, excluded this important aspect in our paper so far, as do many other models in this area.

- Being able to transform our large-scale model to a small-scale model has the advantage that it may be possible to obtain interesting analytical insights. Recall that the dynamics of our small-scale model is due to a (stochastic) map with four different branches. Avrutin et al. (2016) are currently deriving new methods and tools on how to analyze piecewise (deterministic) maps. Related financial market examples include Tramontana et al. (2010) and Huang et al. (2010). Establishing the relation between large-scale models and small-scale models in more detail may thus lead to new analytical results.

- The finding that the performance of the large-scale model is comparable to that of the small-scale model suggests that, in order to improve the performance of the model even further, one should consider different trading rules, more complicated trading rules, or both. Finding the right balance between realism and simplicity will be an important challenge in future agent-based modeling. Medium-scale models may be the answer to this problem.

To conclude, we hope that our paper contributes to a better understanding of the functioning of financial markets and encourages more work in this exciting research direction.

Compliance with Ethical Standards: This study was funded by ISCH COST Action IS1104: "The EU in the new complex geography of economic systems: models, tools, and policy evaluation". The authors declare that they have no conflict of interest.

References

[1] Alfarano S. and Lux T. (2010): Extreme value theory as a theoretical background for power law behavior. Kiel Working Paper 1648, Kiel Institute for the World Economy.

[2] Arifovic, J., Jiang, J. and Xu, Y. (2013): Experimental evidence of bank runs as pure coordination failures. Journal of Economic Dynamics and Control, 37, 2446-2465.

[3] Arifovic, J. and Jiang, J. (2014): Do sunspots matter? Evidence from an experimental study of bank runs. Bank of Canada, Working Paper No. 2014-12.

[4] Avrutin, V., Gardini, L., Schanz, M., Sushko I. and Tramontana, F. (2016): Continuous and discontinuous piecewise-smooth one-dimensional maps: invariant sets and bifurcation structures. World Scientific, Singapore.

[5] Azariadis, C. (1981): Self-fulfilling prophecies. Journal of Economic Theory, 25, 380-396.

[6] Brock, W. and Hommes, C. (1998): Heterogeneous beliefs and routes to chaos in a simple asset pricing model. Journal of Economic Dynamics Control, 22, 1235-1274.

[7] Brock, W., Hommes, C. and Wagener, F. (2005): Evolutionary dynamics in markets with many trader types. Journal of Mathematical Economics, 41, 7-42.

[8] Cass, D. and Shell, K. (1983): Do sunspots matter? Journal of Political Economy, 91, 193-227.

[9] Chen, S.-H. and Yeh, C.-H. (2001): Evolving traders and the business school with genetic programming: A new architecture of the agent-based artificial stock market. Journal of Economic Dynamics and Control, 25, 363-393.

[10] Chen, Z. and Lux, T. (2015): Estimation of sentiment effects in financial markets: A simulated method of moments approach. FinMaP-Working Paper, No. 37, University of Kiel.

[11] Chiarella, C., Dieci, R. and He, X.-Z. (2007): Heterogeneous expectations and speculative behaviour in a dynamic multi-asset framework. Journal of Economic Behavior and Organization 62, 408-427.

[12] Cont, R. (2001): Empirical properties of asset returns: stylized facts and statistical issues. Quantitative Finance, 1, 223-236.

[13] Cont, R. and Bouchaud, J.-P. (2000): Herd behavior and aggregate fluctuations in financial markets. Macroeconomic Dynamics, 4, 170-196.

[14] Cutler, D., Poterba, J. and Summers, L. (1989): What moves stock prices? Journal of Portfolio Management, 15, 4-12.

[15] Day, R. and Huang, W. (1990): Bulls, bears and market sheep. Journal of Economic Behavior and Organization, 14, 299-329.

[16] De Grauwe, P., Dewachter, H. and Embrechts, M. (1993): Exchange rate theory - chaotic models of foreign exchange markets. Blackwell, Oxford.

[17] Diks, C. and van der Weide, R. (2005): Herding, a-synchronous updating and heterogeneity in memory in a CBS. Journal of Economic Dynamics and Control, 29, 741-763.

[18] Duffy, J. and Fisher, E. (2005): Sunspots in the laboratory. American Economic Review, 95, 510-529.

[19] Fair, R. (2002): Events that shook the market. Journal of Business, 75, 713-731.

[20] Farmer, D. and Joshi, S. (2002): The price dynamics of common trading strategies. Journal of Economic Behavior and Organization, 49, 149-171.

[21] Fehr, D., Heinemann, F., Llorente-Saguer, A. (2012): The power of sunspots: an experimental analysis. Federal Reserve Bank of Boston, Working Paper No. 13-2.

[22] Franke, R. (2009a): Applying the method of simulated moments to estimate a small agent-based asset pricing model. Journal of Empirical Finance, 16, 804-815.

[23] Franke, R. (2009b): A prototype model of speculative dynamics with position-based trading. Journal of Economic Dynamics and Control, 33, 1134-1158.

[24] Franke, R. (2010): On the specification of noise in two agent-based asset-pricing models. Journal of Economic Dynamics and Control, 34, 1140-1152.

[25] Franke, R. and Asada, T. (2008): Incorporating positions into asset pricing models with order-based strategies. Journal of Economic Interaction and Coordination, 3, 201-227.

[26] Franke, R. and Westerhoff, F. (2012): Structural stochastic volatility in asset pricing dynamics: estimation and model contest. Journal of Economic Dynamics and Control, 36, 1193-1211.

[27] Franke, R. and Westerhoff, F. (2016) Why a simple herding model may generate the stylized facts of daily returns: explanation and estimation. Journal of Economic Interaction and Coordination, 11, 1-34.

[28] Graham, B. and Dodd, D. (1951): Security analysis. McGraw-Hill, New York.

[29] Gopikrishnan, P., Plerou, V., Amaral, L., Meyer, M. and Stanley, E. (1999): Scaling of the distributions of fluctuations of financial market indices. Physical Revue E, 60, 5305-5316.

[30] Hill, B. (1975): A simple general approach to inference about the tail of a distribution. Annals of Statistics, 3, 1163-1174.

[31] Hommes, C. (2006): Heterogeneous agent models in economics and finance. In: Tesfatsion, L. and Judd, K. (eds.): Handbook of computational economics: agent-based computational economics. North-Holland, Amsterdam, 1109-1186.

[32] Huang, W., Zheng, H. and Chia, W.M. (2010): Financial crisis and interacting heterogeneous agents. Journal of Economic Dynamics and Control, 34, 1105-1122.

[33] LeBaron, B. (2006): Agent-based computational finance. In: Tesfatsion, L. and Judd, K. (eds.): Handbook of computational economics: agent-based computational economics. North-Holland, Amsterdam, 1187-1233.

[34] LeBaron, B. (2009): Robust properties of stock return tails. Brandeis University, Working Paper.

[35] LeBaron, B. (2012): Heterogeneous gain learning and the dynamics of asset prices. Journal of Economic Behavior and Organization, 83, 424-445.

[36] LeBaron, B., Arthur, B. and Palmer, R. (1999): Time series properties of an artificial stock market. Journal of Economic Dynamics and Control, 23, 1487-1516.

[37] Lux, T. (1995): Herd behaviour, bubbles and crashes. Economic Journal, 105, 881-896.

[38] Lux, T. and Marchesi, M. (1999): Scaling and criticality in a stochastic multi-agent model of a financial market. Nature 397, 498-500.

[39] Lux, T. and Ausloos, M. (2002): Market fluctuations I: Scaling, multiscaling, and their possible origins. In: Bunde, A., Kropp, J. and Schellnhuber, H. (eds.): Science of disaster: climate disruptions, heart attacks, and market crashes. Springer: Berlin, 373-410.

[40] Manski, C. and McFadden, D. (1981): Structural analysis of discrete data with econometric applications. MIT Press, Cambridge.

[41] Mantegna, R. and Stanley, E. (2000): An introduction to econophysics. Cambridge University Press, Cambridge.

[42] Marimon, R. and Sunder, S. (1993): Expectationally driven market volatility: an experimental study. Journal of Economic Theory, 61, 74-103.

[43] Murphy, J. (1999): Technical analysis of financial markets. New York Institute of Finance, New York.

[44] Niederhoffer, V. (1971): The analysis of world events and stock prices. Journal of Business, 44, 193-219.

[45] Plerou, V., Gopikrishnan, P., Amaral, L., Meyer, M. and Stanley, E. (1999): Scaling of the distribution of price fluctuations of individual companies. Physical Revue E, 60, 6519-6529.

[46] Raberto, M., Cincotti, S., Focardi, S. and Marchesi, M. (2001): Agent-based simulation of a financial market. Physica A, 299, 319-327.

[47] Schmitt, N. and Westerhoff, F. (2014): Speculative behavior and the dynamics of interacting stock markets. Journal of Economic Dynamics and Control, 45, 262-288.

[48] Schmitt, N. and Westerhoff, F. (2016): Herding behavior and volatility clustering in financial markets. BERG Working Paper No. 107, University of Bamberg.

[49] Shiller, R. (2015): Irrational exuberance. Princeton University Press, Princeton.

[50] Stanley, E., Gabaix, X., Gopikrishnan, P. and Plerou, V. (2007): Economic fluctuations and statistical physics: quantifying extremely rare and less rare events in finance. Physica A, 382, 286-301.

[51] Tramontana, F., Westerhoff, F. and Gardini, L. (2010): On the complicated price dynamics of a simple one-dimensional discontinuous financial market model with heterogeneous interacting traders. Journal of Economic Behavior and Organization, 74, 187-205.

[52] Westerhoff, F. and Dieci, R. (2006): The effectiveness of Keynes-Tobin transaction taxes when heterogeneous agents can trade in different markets: a behavioral finance approach. Journal of Economic Dynamics and Control, 30, 293-322.

[53] Winker, P., Gilli, M. and Jeleskovic, V. (2007): An objective function for simulation based inference on exchange rate data. Journal of Economic Interaction and Coordination, 2, 125-145.

BERG Working Paper Series (most recent publications)

80 Christian **Aßmann**, Assessing the Effect of Current Account and Currency Crises on Economic Growth, May 2011

81 Björn-Christopher **Witte**, Fund Managers – Why the Best Might be the Worst: On the Evolutionary Vigor of Risk-Seeking Behavior, July 2011

82 Björn-Christopher **Witte**, Removing systematic patterns in returns in a financial market model by artificially intelligent traders, October 2011

83 Reiner **Franke** and Frank **Westerhoff**, Why a Simple Herding Model May Generate the Stylized Facts of Daily Returns: Explanation and Estimation, December 2011

84 Frank **Westerhoff**, Interactions between the real economy and the stock market, December 2011

85 Christoph **Wunder** and Guido **Heineck**, Working time preferences, hours mismatch and well-being of couples: Are there spillovers?, October 2012

86 Manfred **Antoni** and Guido **Heineck**, Do literacy and numeracy pay off? On the relationship between basic skills and earnings, October 2012

87 János **Seregi**, Zsuzsanna **Lelovics** and László **Balogh**, The social welfare function of forests in the light of the theory of public goods, October 2012

88 Frank **Westerhoff** and Reiner **Franke**, Agent-based models for economic policy design: two illustrative examples, November 2012

89 Fabio **Tramontana**, Frank **Westerhoff** and Laura **Gardini**, The bull and bear market model of Huang and Day: Some extensions and new results, November 2012

90 Noemi **Schmitt** and Frank **Westerhoff,** Speculative behavior and the dynamics of interacting stock markets, November 2013

91 Jan **Tuinstra**, Michael **Wegener** and Frank **Westerhoff,** Positive welfare effects of trade barriers in a dynamic equilibrium model, November 2013

92 Philipp **Mundt**, Mishael **Milakovic** and Simone **Alfarano,** Gibrat's Law Redux: Think Profitability Instead of Growth, January 2014

93 Guido **Heineck**, Love Thy Neighbor – Religion and Prosocial Behavior, October 2014

94 Johanna Sophie **Quis**, Does higher learning intensity affect student well-being? Evidence from the National Educational Panel Study, January 2015

95 Stefanie P. **Herber**, The Role of Information in the Application for Merit-Based Scholarships: Evidence from a Randomized Field Experiment, January 2015

96 Noemi **Schmitt** and Frank **Westerhoff**, Managing rational routes to randomness, January 2015

97 Dietmar **Meyer** and Adela **Shera**, Remittances' Impact on the Labor Supply and on the Deficit of Current Account, February 2015

98 Abdylmenaf **Bexheti** and Besime **Mustafi**, Impact of Public Funding of Education on Economic Growth in Macedonia, February 2015

99 Roberto **Dieci** and Frank **Westerhoff**, Heterogeneous expectations, boom-bust housing cycles, and supply conditions: a nonlinear dynamics approach, April 2015

100 Stefanie P. **Herber**, Johanna Sophie **Quis**, and Guido **Heineck**, Does the Transition into Daylight Saving Time Affect Students' Performance?, May 2015

101 Mafaïzath A. **Fatoke-Dato**, Impact of an educational demand-and-supply policy on girls' education in West Africa: Heterogeneity in income, school environment and ethnicity, June 2015

102 Mafaïzath A. **Fatoke-Dato**, Impact of income shock on children's schooling and labor in a West African country, June 2015

103 Noemi **Schmitt**, Jan **Tuinstra** and Frank **Westerhoff**, Side effects of nonlinear profit taxes in an evolutionary market entry model: abrupt changes, coexisting attractors and hysteresis problems, August 2015.

104 Noemi **Schmitt** and Frank **Westerhoff**, Evolutionary competition and profit taxes: market stability versus tax burden, August 2015.

105 Lena **Dräger** and Christian R. **Proaño**, Cross-Border Banking and Business Cycles in Asymmetric Currency Unions, November 2015.

106 Christian R. **Proaño** and Benjamin **Lojak**, Debt Stabilization and Macroeconomic Volatility in Monetary Unions under Heterogeneous Sovereign Risk Perceptions, November 2015.

107 Noemi **Schmitt** and Frank **Westerhoff**, Herding behavior and volatility clustering in financial markets, February 2016

108 Jutta **Viinikainen**, Guido **Heineck**, Petri **Böckerman**, Mirka **Hintsanen**, Olli **Raitakari** and Jaakko **Pehkonen**, Born Entrepreneur? Adolescents' Personality Characteristics and Self-Employment in Adulthood, March 2016

109 Stefanie P. **Herber** and Michael **Kalinowski**, Non-take-up of Student Financial Aid: A Microsimulation for Germany, April 2016

110 Silke **Anger** and Daniel D. **Schnitzlein**, Cognitive Skills, Non-Cognitive Skills, and Family Background: Evidence from Sibling Correlations, April 2016

111 Noemi **Schmitt** and Frank **Westerhoff**, Heterogeneity, spontaneous coordination and extreme events within large-scale and small-scale agent-based financial market models, June 2016